Preparation and characterization of Pd/C catalyst obtained in NH₃-mediated polyol process

Huanqiao Li [a,b], Gongquan Sun [a,*], Qian Jiang [a,b],
Mingyuan Zhu [a,b], Shiguo Sun [a], Qin Xin [a,c]

[a] *Direct Alcohol Fuel Cell Laboratory, Dalian Institute of Chemical Physics, Chinese Academy of Sciences,*
457 Zhongshan Road, Dalian 116023, China
[b] *Graduate School of the Chinese Academy Sciences, Beijing 100039, China*
[c] *State Key Laboratory of Catalysis, Dalian Institute of Chemical Physics, Chinese Academy of Sciences, Dalian 116023, China*

Abstract

Vulcan XC-72R carbon supported Pd nanoparticles was obtained in a NH₃-mediated polyol process without any protective agent and characterized by X-ray diffraction (XRD) and transmission electron microscope (TEM) techniques. The added NH₃ species is found to have a strong complex ability to Pd, which not only avoids the formation of Pd hydroxide precipitate resulted from Pd hydrolysis, but also restrains the further complete reduction of Pd. Temperature-programmed reduction equipped with a mass spectrometry (TPR-MS) is employed to study the reductive behavior of unreduced Pd complex in Pd/C catalyst and the results show that the post-treatment in a reductive atmosphere at higher temperature is needed to ensure the complete reduction of Pd. XRD patterns show the heat-treated Pd/C sample in a reductive atmosphere has a face centered cubic crystal structure and TEM image indicates that the dispersion of Pd nanoparticles on the carbon support is uniform and in a narrow particle size range. Thermodynamic data analysis is carried out to elucidate the possible reaction pathway for the preparation of Pd/C catalyst in this process. The obtained Pd/C catalyst shows high activity to formic acid oxidation and high selectivity to oxygen reduction reaction (ORR) with the presence of methanol.

1. Introduction

Metal/carbon nanocomposites consisting of metal nanoparticles supported on a carbon powder of high surface area are commonly employed as heterogeneous catalysts in both small- and large-scale chemical processes. In the literatures, great interest has been placed on the use of carbon supported Pd nanoparticles as effective catalysts for many organic and inorganic reactions [1,2]. In addition, they may be alternative catalysts with respect to Pt metal in low temperature proton exchange membrane fuel cell (PEMFC) due to their unique properties. As reported in recent work, nanosized Pd catalysts have been considered to be potential anode materials for direct formic acid fuel cell (DFAFC) due to their high catalytic activity to formic acid oxidation at lower temperature [3–5]. The anodic oxidation of formic acid on Pd-based catalysts has been proposed to occur via a direct pathway, in which formic acid is directly oxidized to form the final product of CO_2 without forming CO like intermediate. In comparison with Pt-based catalysts, on which formic acid is oxidized to CO_2 with poisoning CO as the main reactive intermediate, the adoption of Pd catalyst could enhance the formic acid oxidation activity and decrease CO poisoning of the electrode catalyst, and thus to enhance cell performance of a DFAFC greatly [3]. Another interesting property of Pd catalyst is its high sensitivity to oxygen reduction reaction (ORR) in acid solution with the presence of methanol. The methanol crossover is considered to be one of the biggest problems for the further development of direct methanol fuel cell (DMFC) technology. The crossover methanol in the cathode side is well known to depolarize the cathode greatly and

---

* Corresponding author. Tel.: +86 411 84379063; fax: +86 411 84379063.
  E-mail address: gqsun@dicp.ac.cn (G. Sun).

result in a substantial loss of DMFC cell performance. It had been reported that ORR proceeded on Pd via a 4e pathway, similar to the case on Pt metal [6]. But Pd shows a different electrochemical behavior from Pt metal with respect to methanol oxidation in that Pd is less active for methanol electro-oxidation in acid solution [7]. Pd-based Pd–Fe/C and Pd–Co/C catalysts have been proved to possess high selectivity to ORR in presence of methanol in comparison with Pt-based catalysts [8–10]. This implies that Pd nanoparticles show a potential application in the future development of low temperature direct liquid fuel cell technology.

The smaller sized Pd nanoparticles with higher Pd metal utilization have been found to be much more active than the bigger ones in the literatures [5]. Thus, various methods have been employed to obtain highly active Pd/C catalyst with smaller sized Pd nanoparticles. Among these methods, liquid phase-based chemical reduction route is mostly preferred because it is simple and economical, and can realize better size and size distribution control by optimizing the experimental parameters. To prevent aggregation, metal nanoparticles are often prepared in the solution with the presence of long chains surfactants and polymers with specific donor atoms or chemical groupings such as polyvinylpyrrolidones (PVP), polyvinyl alcohol (PVA) and polyacrylic acid (PAA) as protective agents [11–15]. The Pd metal salt precursors usually form a complex with the surfactant before the reduction reaction is carried out. The resulting metal colloid is then stabilized by hydrophobic interactions between hydrophobic segments of the polymers and surface of the metal colloid. However, these stabilizers usually adsorb strongly onto the Pd nanoparticles surface, which may decrease the catalytic activity and selectivity of the metal nanoparticles greatly, especially for their application in the electrochemical catalytic area due to the low conductivity of long chain polymers [16,17]. To avoid this strong adsorption effect of the stabilizers, some researchers have modified the polyol process in ethylene glycol solution and obtained highly dispersed Pt/C and PtRu/C electro-catalysts [18,19]. However, there is few report on the preparation of highly dispersed Pd/C catalyst in the absence of surfactant agents or template materials. Our previous study has shown that the addition of NH_3 species in the polyol process could facilitate formation of highly dispersed Pd/C electro-catalyst without using any surfactant agent [20]. In this study, the possible evolved reaction pathway during the preparation of Pd/C catalyst in the NH_3-mediated polyol process in ethylene glycol solution will be elucidated in detail.

2. Experimental

2.1. Catalyst preparation

The preparation of Pd/C catalyst with a Pd metal loading of 30% was carried out by a NH_3-mediated polyol process which has been described in detail as follows. At first, Vulcan XC-72R carbon black was pre-treated with 5 M HCl and 2 M HNO_3 solutions under refluxing condition to remove some ash before being suspended in ethylene glycol solution [21]. The calcu-

lated amount of $PdCl_2$ was dissolved in 80 mL ethylene glycol under ultrasonic stirring with the help of dilute hydrochloric acid (HCl, 1 mol L^{-1}) at room temperature. Two milliliters of aqueous ammonia (37%, v/v) was introduced to $PdCl_2$ solution and the color of the solution changed from yellow to colorless, demonstrating the formation of Pd–NH_3 complex. After stirring for 30 min, pH scale of the mixture was adjusted to 12–13 using 4 mL aqueous NaOH solution (1 mol L^{-1}), which was followed by addition of the pre-dispersed carbon ink. The resulted mixture was stirred for over 30 min and was heated slowly up to 130 °C in half an hour. The high temperature aging at 130 °C lasted 3 h. After cooling to the ambient temperature, the liquid solvent was removed by distillation in vacuum. The system temperature was controlled at 130 °C and the pressure was fixed at 10 mmHg. The resulted powder was then dried in a vacuum oven at 100 °C overnight and denoted as Pd/C-N-a.

The obtained Pd/C-N-a sample was subjected to heat-treatments under different atmospheres at elevated temperatures. In a typical operation, about 100 mg of Pd/C-N-a sample was filled in a quartz boat and was placed into a quartz tube on a homemade tube furnace instrument. The quartz tube loaded with the catalyst was firstly degassed by high purity Ar gas at 120 °C for 1 h. After the quartz tube was refilled with high purity Ar gas, the flow rate of the gas was fixed at 30 mL min^{-1} and the temperature of the oven was increased at a rate of 10 °C min^{-1} till 300 °C and then lasted 2 h. Afterwards, the oven was removed off and the catalyst was allowed to cool down to room temperature in an inert atmosphere to avoid inflammation. The resulted powder was washed with hot distilled water to remove chloride and other impurities and then dried in a vacuum oven at 70 °C overnight, and denoted as Pd/C-N-a-300Ar. For heat-treatments of the catalyst under a reductive atmosphere, the quartz tube was switched to H_2–Ar gas mixture (1/9, v/v) channel after degasification with high purity Ar gas. Then, the oven was heated to the desired temperature at a rate of 10 °C min^{-1} and lasted for 2 h. By a sequence of washing and drying, the sample was denoted as Pd/C-N-a-300H when the heat-treatment temperature was 300 °C and as Pd/C-N-a-500H when the temperature was 500 °C.

For comparison, Pd/C sample in a polyol process without the mediation of NH_3 was also prepared by the polyol process method in ethylene glycol solution. In brief, the pre-treated carbon support (200 mg) was suspended in 50 mL ethylene glycol under ultrasonic stirring, and then the precursor of $PdCl_2$ solution was added dropwise to the carbon ink in 30 min. After stirring for another 30 min, suitable amount NaOH solution (1 mol L^{-1}) was added to adjust pH scale of the mixture to 12–13. The reduction reaction was performed by heating the solution at 130 °C for 3–4 h. After cooled down to the room temperature, the resulted powder was washed with hot distilled water to remove chloride until no chloride anion in the filtrate was detected with $AgNO_3$ solution (1 mol L^{-1}). Then the obtained catalyst was dried in a vacuum oven at 70 °C overnight and denoted as Pd/C-b. In the same way, Pt/C sample with 40% metal loading was also obtained in this polyol process and denoted as Pt/C-b.

2.2. Catalyst characterizations

2.2.1. Transmission electron microscope (TEM)

The morphology and dispersion of the catalysts were examined by TEM on a JEOL JEM-2000EX electron microscope operated at 100 kV with a magnification of 250,000×. For the microscopic examinations, about 5 mg sample was firstly ultrasonically dispersed in ethanol and then one drop of the catalyst ink was deposited on a copper grid covered by carbon film. The size distribution of the metal nanoparticles in the supported catalysts was obtained by directly measuring the size of 300 randomly chosen particles in the TEM images.

2.2.2. X-ray diffraction (XRD)

The characteristics of the crystalline structure of these supported catalysts were determined using the powder XRD technique. The data was obtained using a Rigaku D/MAX 2500 X-ray power diffractometer with a Cu Kα radiation source ($\lambda = 1.54056$ Å) and a Ni filter. About 30 mg powdered electrocatalyst sample was kept in a quartz block and pressed onto the quartz block using a glass slide to obtain a uniform distribution. The 2θ Bragg angles were scanned over a range of 15–85° at a rate of 5° min^{-1} with a 0.02° angular resolution. The tube current was 100 mA and the tube voltage was 40 kV. Scherrer and Bragg formula were employed to calculate mean diameter and lattice parameter of the catalysts [22].

2.2.3. Temperature-programmed reduction with a mass spectrometry (TPR-MS) characterization of Pd/C-N-a

TPR-MS characterization of Pd/C-N-a sample was carried out on an Auto-chem 2910 instrument to detect the unreduced Pd species in a reductive atmosphere. For the TPR-MS run, 43.9 mg of Pd/C-N-a was loaded into a U-type quartz tube. The reactor was then purged with an Ar flow (40 mL min^{-1}) at the temperature of 120 °C for 30 min for water removal. When the temperature of the reactor was cooled to room temperature, high purity Ar gas was replaced by H$_2$/He mixture (1/9, v/v) and the flow rate of the mixture gas was controlled at 10 mL min^{-1}. The temperature of the reactor was increased programmed from room temperature to 520 °C with a heating rate of 10 °C min^{-1}. Meanwhile, mass spectroscopy (MS) was employed to detect the reaction product during the TPR measurement of Pd/C-N-a sample.

2.2.4. Electrochemistry measurement

A CHI 760B potentistat/galvanostat was used for the cyclic voltammetry (CV) measurements in a standard three-compartment electrochemical cell. The working electrode was a glass carbon disk with a diameter of 4 mm held in a Teflon cylinder. A Pt-foil counter-electrode and a saturated calomel reference electrode (SCE), which was connected to the electrochemical cell by a KNO$_3$ salt bridge, were used. All potentials in this work were referred to normal hydrogen electrode (NHE). The CV experiments were carried out at 25 ± 0.5 °C in 0.5 M HClO$_4$ solution saturated with high purity N$_2$. Thin porous coating disk electrodes design had been described in previous work [23]. Five milligrams of catalyst was ultrasonically suspended

with 2 ml ethanol and 50 μL 5 wt.% Nafion® solution (Du Pont, USA) for 30 min to obtain uniformly catalyst paint, then 10 μL of the catalyst ink was spread on the surface of clean glass carbon electrode with a micropipette. The solvent was removed by evaporating at room temperature for 30 min. Solution of 0.5 M HClO$_4$ was prepared from high purity acid and triply distilled water. Before each measurement, fast potential pulses (100 mV s^{-1}) between 0 and 1200 mV was applied to the electrodes for surface cleaning and obtaining a reproductive curve. CV curves were recorded in a potential pulse at a scan rate of 50 mV s^{-1}.

The activity evaluation of Pd/C catalyst to formic acid oxidation or methanol oxidation was carried out in 0.5 M HClO$_4$ electrolyte containing 1 M HCOOH (or 1 M CH$_3$OH) by employing the electrochemical equipment of CHI 760B potentistat/galvanostat at 25 ± 0.5 °C.

For the examination of ORR on Pd/C in the presence of methanol, methanol reagent was added to oxygen saturated base electrolyte to obtain the required concentration of 0.1 M. Voltammetry curves were recorded in a negative potential sweep at a scan rate of 10 mV s^{-1}. The rotation speed of the rotating disk electrode (RDE) was fixed at 1600 rpm to decrease the O$_2$ mass transfer in the solution.

3. Results and discussion

3.1. TEM characterization

Fig. 1 shows the TEM images of Pd/C-b and Pt/C-b samples obtained from the polyol process in ethylene glycol (EG) solution. It is clearly found that there are heavy agglomerations of Pd nanoparticles in Pd/C-b sample; while for Pt/C-b catalyst, highly dispersed Pt nanoparticles with an average diameter of 3.0 nm are uniformly supported on the carbon surface. This indicates that the polyol process in EG solution presents large advantages in the preparation of highly dispersed Pt nanoparticles; which has been proved in previous work [18,19,24]. However, for Pd nanoparticles, it is difficult to avoid the agglomeration of Pd nanoparticles if no surfactant agent is employed during the catalyst preparation. This is because Pd is one of the strongest hydrolysable metals. Highly insoluble hydroxides are usually formed during Pd catalyst preparation, which results in the serious agglomeration of Pd nanoparticles, as shown in Fig. 1a. To obtain Pd/C catalyst with a better Pd nanoparticles dispersion, NH$_3$ species has been introduced during catalyst preparation because NH$_3$ is well known to have a strong complex ability to Pd and can be easily removed by post-treatment at higher temperature. TEM image of the as-received Pd/C-N-a obtained in NH$_3$-mediated polyol process is shown in Fig. 2a and it shows no serious agglomeration of Pd nanoparticles on carbon support. But, it should be noted that the TEM image of Pd/C-N-a mostly resembles the characteristic of Vulcan XC-72R carbon support (shown in Fig. 2e), with only a few tiny metal nanoparticles observed on carbon support. This is possibly because the reduction ability of ethylene glycol is relatively weak in comparison with other powerful reducing agents like sodium borohydride and cannot reduce the strong complex Pd–NH$_3$ completely, and thus results in a large amount of unreduced amorphous Pd com-
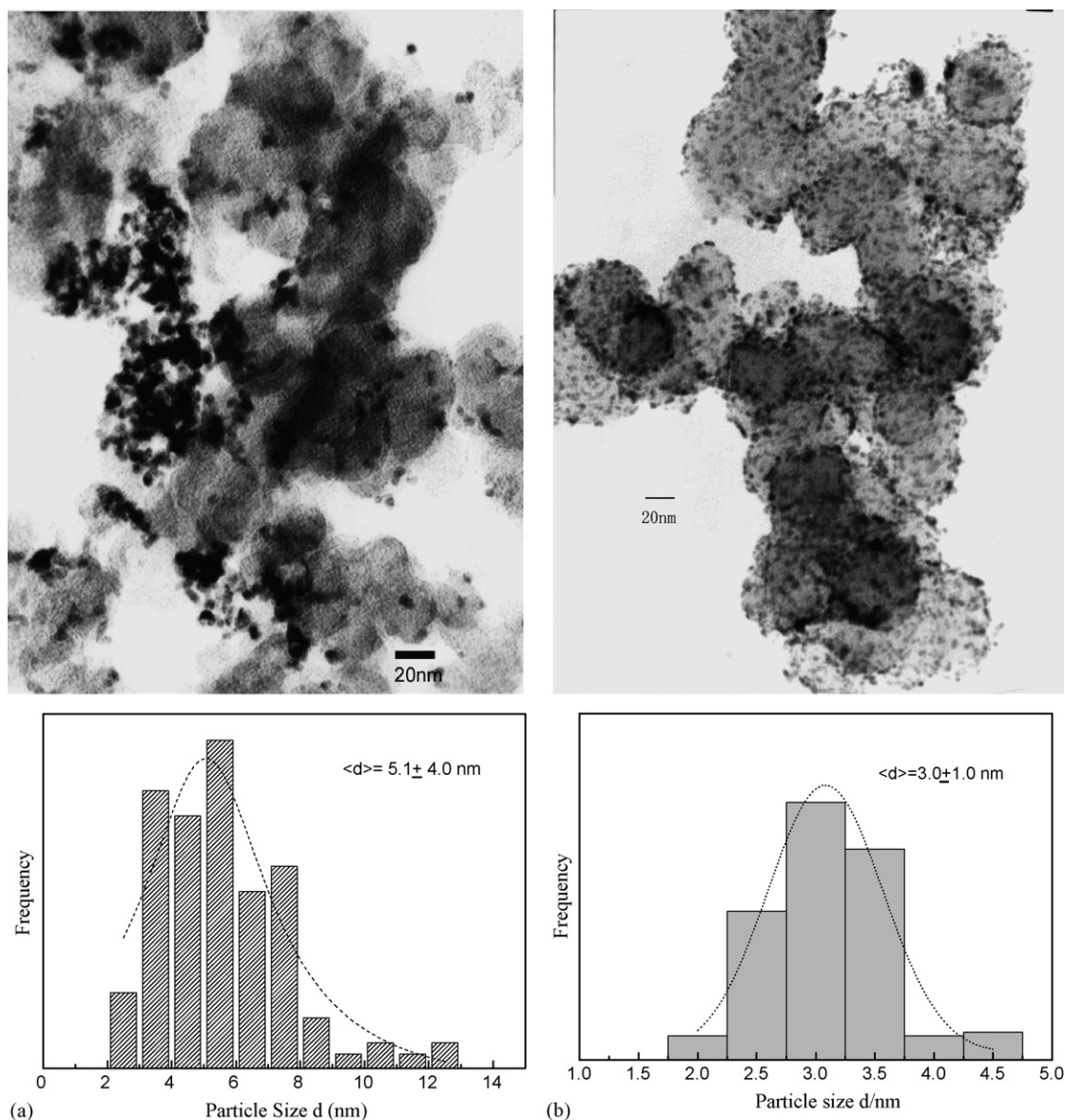
Fig. 1. TEM images and size distributions of Pd/C-b (a) and Pt/C-b (b) obtained from a polyol process in ethylene glycol solution without any protective agent.

pounds in the catalyst. Further treatment in an inert atmosphere at the elevated temperature of 300 °C could induce growth up of the smaller Pd nanoparticles in Pd/C-N-a sample, as displayed in Fig. 2. The mean particle size is enlarged to 3.0 nm in the range of 1.5–5 nm, but the amount of unreduced Pd complex remains unchanged. To obtain highly dispersed Pd/C catalyst with high amount of reduced Pd(0) species, the post-treatment of Pd/C-N-a sample in a reductive atmosphere is carried out to ensure complete reduction of Pd. TEM images of Pd/C-N-a-300H and Pd/C-N-a-500H, which are obtained by the post-treatment of Pd/C-N-a sample in a reductive atmosphere, are shown in Fig. 2c and d. It can be found that large quantities of Pd nanoparticles are emerged on the carbon support with uniform distribution. The mean diameter of Pd/C-N-a-300H is about 3.4 nm with a distribution of 1.5–5 nm, which is analogous to that of Pd/C-N-a-300Ar. When the temperature is increased to 500 °C, the mean particle size is increased to 5.2 nm with a distribution of

2–10 nm and the dispersion of Pd nanoparticles in Pd/C-N-a-500H is deteriorated to some extent due to higher temperature treatment. This also indicates that treatment temperature has a much more important effect on the dispersion state of metal nanoparticles for the supported catalysts than the atmosphere.

The corresponding weight losses of the Pd/C-N-a under different atmospheres were also recorded and are illustrated in Table 1. For comparison, the weight losses of Pt/C-b and Pd/C-b catalysts undergone the same heat-treatments are also included. It can be found from Table 1 that the weight losses of the samples are affected both by the atmospheres and temperatures. For Pt/C-b and Pd/C-b samples, the weight losses are about 2.6% and 2.7% in an inert atmosphere at 500 °C, which is mainly resulted from the loss of water in the samples [25]. When the samples are heat-treated in a reductive atmosphere, the weight losses are enlarged to 5% and 6.6%, respectively. The relatively bigger weight losses of the samples in a reductive atmosphere
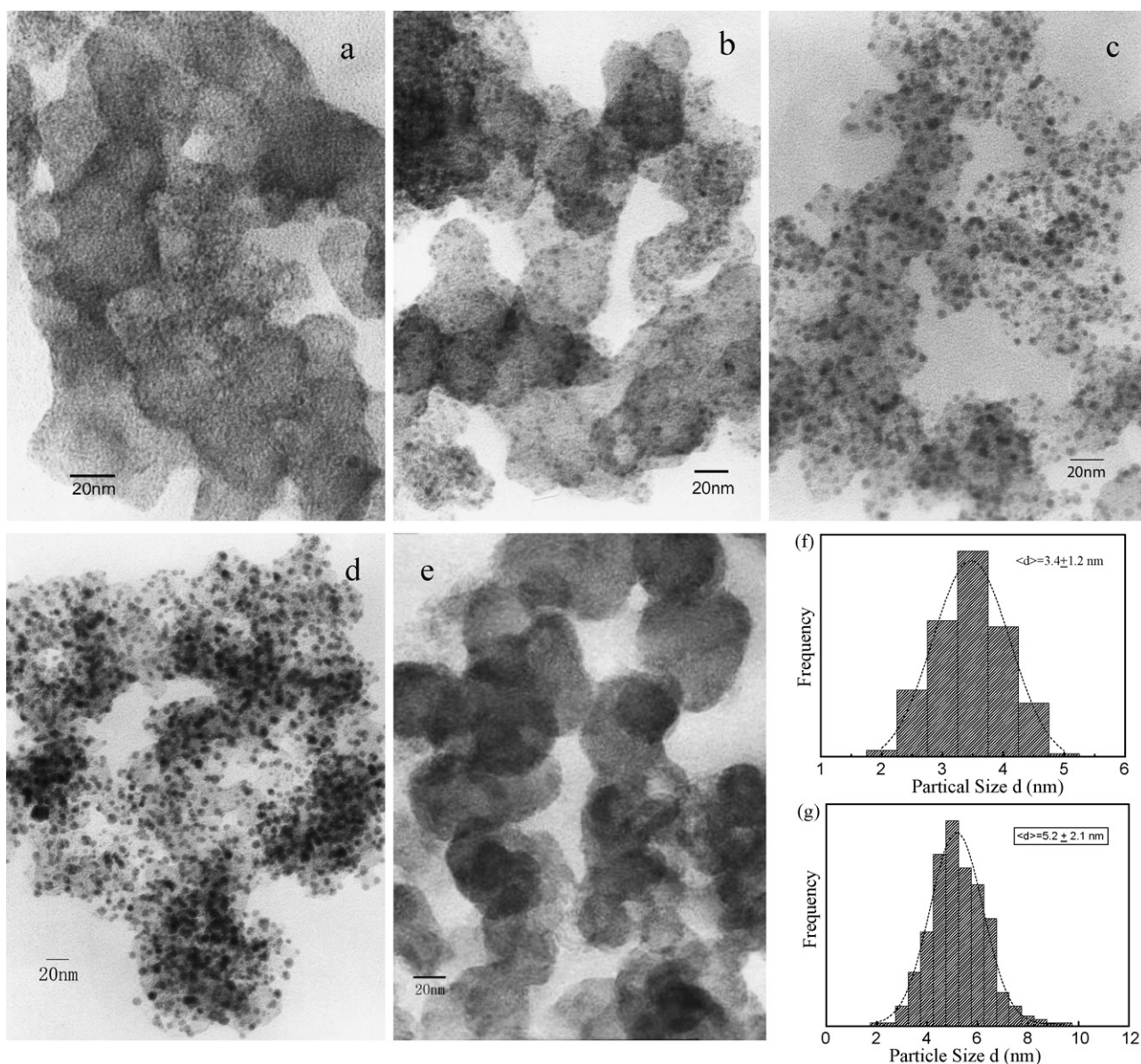
Fig. 2. TEM images of Pd/C obtained in a NH$_3$-mediated polyol process after the corresponding heat-treatment: Pd/C-N-a (a); Pd/C-N-a-300Ar (b); Pd/C-N-a-300H (c); Pd/C-N-a-500H (d) and the Vulcan XC-72R carbon support (e). The size distributions of Pd/C-N-a-300H (f) and Pd/C-N-a-500H (g) are also included.

Table 1
Weight losses of the catalysts during the post-treatment in different atmospheres

	Before treatment (mg)	After treatment (mg)	Mass loss (%)
Pd/C-N-a			
Ar treatment (300 °C)	100	90	10
H$_2$ treatment (300 °C)	100	78	22
Ar treatment (500 °C)	100	90	10
H$_2$ treatment (500 °C)	100	78	26
Pd/C-b			
Ar treatment (500 °C)	100	97.3	2.7
H$_2$ treatment (500 °C)	100	93.4	6.6
Pt/C-b			
Ar treatment (500 °C)	100	97.4	2.6
H$_2$ treatment (500 °C)	100	95.0	5

possibly originates from water evaporation, which is resulted from the reduction reaction of a small quantity of metal oxide in the catalysts, or the catalytic hydrogenation of carbon support in presence of Pt or Pd catalyst. However, for Pd/C-N-a sample, the weight loss in inert atmosphere at 300 °C is about 10%, which is much higher than that of Pt/C-b or Pd/C-b. This big weight loss of Pd/C-N-a in inert atmosphere should be ascribed to the volatilization of water or ammonia like species in the sample. And when Pd/C-N-a was heat-treated in a reductive atmosphere at the same temperature, the weight loss is even enlarged to 22%. The big differences of the weight loss of Pd/C-N-a sample in inert and reductive atmosphere are mainly ascribed to the reduction of large amount of unreduced Pd compounds. Due to the strong complex ability of NH$_3$ to Pd, the formed Pd–NH$_3$ complex in NH$_3$-mediated polyol process is difficult to be reduced by ethylene glycol. Only when the sample is heat-treated in a reduc-
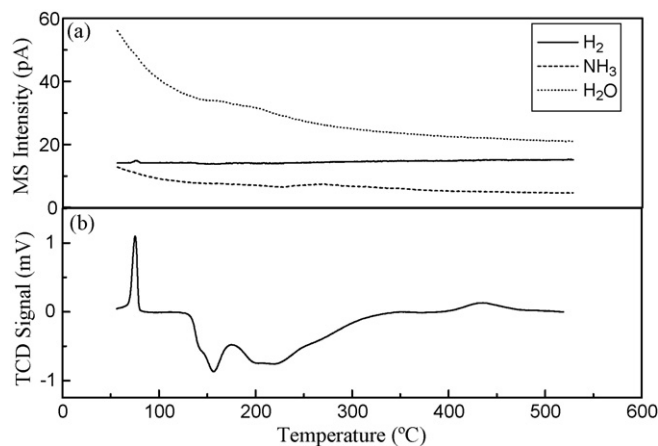
Fig. 3. Temperature-programmed reduction (TPR) (a, up) equipped with mass spectra (b, down) of Pd/C-N-a in H_2/Ar (1/9, v/v) atmosphere at $10\,^{\circ}C\,min^{-1}$.

Fig. 4. XRD patterns of carbon support (a) and Pd/C obtained in a NH_3-mediated polyol process after the corresponding post-treatment: Pd/C-N-a (b), Pd/C-N-a-300Ar (c) and Pd/C-N-a-300H (d). Pd/C-b (e) is also included for comparison.

tive atmosphere at higher temperature, the stable Pd complex could be reduced mostly and thus to result in the big weight loss ratio up to 22%. When the temperature is increased to 500 °C, the weight loss for Pd/C-N-a is only increased to 26%. Combined with TEM results, it can be inferred that most of the Pd compound in Pd/C-N-a could be reduced at 300 °C for 2 h.

3.2. TPR-MS characterization

To explore the reduction behavior of Pd/C-N-a sample under a reductive atmosphere in detail, TPR-MS characterization is carried out in a H_2/Ar gas mixture (1/9, v/v) atmosphere and the corresponding results are displayed in Fig. 3. As shown by TPR spectrum, except for a small H_2 spillover peak below 100 °C, the large H_2 consumption peak starting at 120 °C and ending at 350 °C is mainly due to the reduction of Pd compounds. The H_2 spillover peak at lower temperature originates from the desorption of H_2 from the Pd nanoparticles. By analyzing the results of TPR and on-line mass spectrum, it is found that the reduction product of Pd/C-N-a is mainly consists of H_2O during the initial reduction stage at 150 °C, which is originated from the reduction of $[Pd(OH)_x]^{2-x}$ like compounds. With temperature increased, the amount of the reduction product of NH_3 has reached its peak value at 280 °C, indicating the presence of $[Pd(NH_3)_x]^{2+}$ like compounds. The reduction temperature of $[Pd(NH_3)_x]^{2+}$ is a little higher than that of $[Pd(OH)_x]^{2-x}$, which is mainly attributed to the stronger complex ability of NH_3 than OH^-. In addition, it should be noted that the amount of the reduction product of H_2O and NH_3 are much smaller than their corresponding baseline values, as shown in Fig. 3b, which maybe indicates that much more NH_3 and H_2O are existed in Pd/C-N-a sample than their stoichiometric ratios with Pd. This point is consistent with the above-mentioned big weight loss of the sample during catalyst post-treatment in inert atmosphere.

3.3. XRD characterization

XRD characterization of these samples is carried out to determine the crystal structures and the results are displayed in Fig. 4.
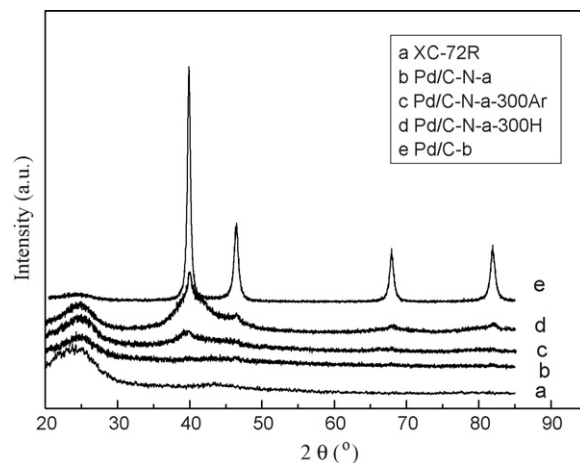
The corresponding XRD patterns of Pd/C-N-a sample resemble only the features of the carbon support, which is consistent with TEM results. The particle size of Pd nanoparticles in Pd/C-N-a sample is too small and the amount is low, which makes it difficult to be detected. When Pd/C-N-a sample is heat-treated at elevated temperature, Pd/C-N-a-300Ar and Pd/C-N-a-300H represent similar diffraction features to polycrystalline Pd of face centered cubic crystal (fcc) structure. The only difference between XRD pattern of Pd/C-N-a-300Ar and Pd/C-N-a-300H sample is the diffraction intensity of Pd characteristic peaks if the carbon support is considered as reference. The diffraction intensity of Pd/C-N-a-300H is much stronger than Pd/C-N-a-300Ar, indicating that the amount of the reduced Pd(0) species in Pd/C-N-a-300H is much higher than in an inert atmosphere. This result is well consistent with TEM images, which indicates that very tiny amorphous Pd nanoparticles can be formed in NH_3-mediated polyol process; however, the size of the nanoparticles is too small and the amount is too low, to be detected by XRD technique. When the sample is heat-treated in an inert atmosphere, tiny nanoparticles could agglomerate into the bigger ones. However, due to strong complex ability of NH_3 to Pd, only a small amount of Pd could be reduced to Pd(0) to result in relatively lower intensity of XRD patterns for Pd/C-N-a-300Ar. Heat-treatment of Pd/C-N-a in a reductive atmosphere could help the complete reduction of Pd. In addition, in comparison with XRD pattern of Pd/C-b sample, the width of the corresponding diffraction peaks of Pd/C-N-a-300H are much broader, indicating the presence of much smaller size of Pd nanoparticles. Based on X-ray line broad method, the mean particle size of Pd/C-N-a-300H is 3.4 nm, which is much smaller than 10.7 nm of Pd/C-b sample.

Based on the above TEM, TPR-MS and XRD characterizations, the reaction pathway of the preparation of Pd/C catalyst in NH_3-mediated polyol process could be put forward in detail here. For better comparison, the synthesis routes of the preparation of Pd/C catalyst in the polyol process with/without the addition of NH_3 species are presented together in Scheme 1. The corresponding changes of Gibbs free energy (ΔG) of the
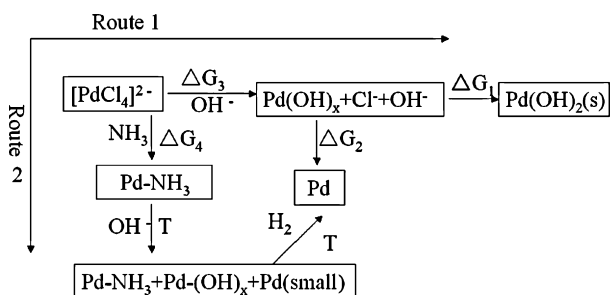
Scheme 1. Reaction routes of Pd/C catalyst preparation with/without NH$_3$ mediation in a polyol process.

possible evolved process in these two routes are calculated and listed in Table 2. Previous work on the preparation of metal nanoparticles catalysts in the polyol process has proved that the presence of a suitable amount of free OH$^-$ ions in the solution could help improving the reduction rate of the noble metal ions and stabilizing the resulted metal colloids to avoid employment of the protective agents [18,19]. However, in case of preparation of Pd nanoparticles, it is found that Pd has a strong tendency to be deposited as Pd(OH)$_x$, as mentioned in Section 2, which is consistent with thermodynamic data analyses. As displayed in Table 2, the Gibbs energy change of Pd(OH)$_x$ formation (-157.5 kJ mol^{-1}) is much more negative than that of the reduction of Pd(OH)$_x$ (-13.5 kJ mol^{-1}) in EG solution, indicating that precipitation of Pd(OH)$_2$ prevails over its reduction reaction. The precipitation of Pd(OH)$_x$ could be reduced by EG with time prolonged. However, the agglomeration of Pd nanoparticles could not be avoided due to Pd(OH)$_2$ precipitation.

While in NH$_3$ modified polyol process, the Gibbs energy change of the formation of [Pd(NH$_3$)$_4$]$^{2+}$ (-118.6 kJ mol^{-1}) is a little more negative than that of the formation of Pd(OH)$_2$ (-106.7 kJ mol^{-1}), indicating that NH$_3$ has a more strong complex ability to Pd to avoid the formation of precipitation of Pd(OH)$_x$. However, there is still small Pd(OH)$_2$ that could be formed due to the similar complex ability of NH$_3$ and OH$^-$ to Pd. Meanwhile, due to strong complex ability of NH$_3$ to Pd, it is difficult to reduce Pd compound to the reduced Pd(0) species. As illustrated in the XRD and TEM results, only very low amount of Pd(0) could be formed. To ensure the reduction of Pd–NH$_3$ complex completely, heat-treatment in a reductive atmosphere is needed, as discussed above.

Table 2
Calculated thermodynamic data of the changes of Gibbs free energy (ΔG) evolved in the different reaction routes

	Changes of Gibbs free energy (kJ mol^{-1})
Route 1	
ΔG_1	-157.5
ΔG_2	-13.5
ΔG_3	-106.7
Route 2	
ΔG_3	-106.7
ΔG_4	-118.6

K_{sp}(Pd(OH)$_2$) = 3×10^{-28}; E(Pd^{2+}/Pd) = 0.915 V.

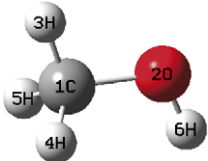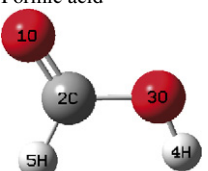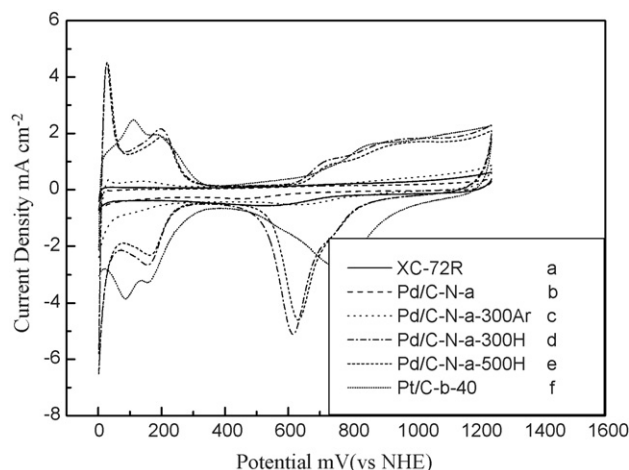Fig. 5. Base cyclic voltammogram curves in 0.5 M HClO$_4$ of carbon support (a) and Pd/C obtained in a NH$_3$-mediated polyol process after the corresponding heat-treatment: Pd/C-N-a (b), Pd/C-N-a-300Ar (c), Pd/C-N-a-300H (d) and Pd/C-N-a-500H (e). Pt/C-b (f) is also included for comparison.

3.4. Electrochemistry test

Cyclic voltammetry method is employed to characterize the electrochemistry property of the prepared Pd/C catalyst. Fig. 5 shows that the base CV curves of these Pd/C catalysts in 0.5 M HClO$_4$ at room temperature (25 ± 0.5 °C). The base CV curves of the carbon support and Pt/C-b are also included. In consistent with XRD and TEM results, CV curve of Pd/C-N-a sample only represents the features of the carbon support. For Pd/C-N-a-300Ar sample, the CV feature resembles a little similar to polycrystalline Pd in acid solution, but the intensity is too weak, indicating the presence of low amount of reduced Pd(0) species. After Pd/C-N-a is reduced in a reductive atmosphere at elevated temperature, CV curves of Pd/C-N-a-300H and Pd/C-N-a-500H display the main characteristic of polycrystalline Pd in acid solution [26]. The sharp peak from 0 to 150 mV is mainly originated from the oxidation of the β-phase of absorbed hydrogen, which is totally different from the CV feature of Pt. On Pt/C-b catalyst, three resolved peaks in hydrogen adsorption–desorption region can be clearly resolved which are associated with weakly and strongly bonded hydrogen species on different crystal faces of Pt nanoparticles. By comparing the CV curves of Pd/C-N-a-300H with Pd/C-N-a-500H samples, it can be found that heat-treatment in a H$_2$/Ar reductive atmosphere at the lower temperature facilitates the formation of small Pd nanoparticles with bigger hydrogen adsorption–desorption region area, which is an indication of bigger electrochemistry surface area to some extent.

The activity of Pd/C catalyst to HCOOH oxidation has been evaluated in previous work [20]. As respect to CH$_3$OH oxidation, it is found that the obtained Pd/C-N-a-300H catalyst exhibits much lower activity than Pt/C-b. Fig. 6 compares CV curves of methanol oxidation obtained in 0.5 M HClO$_4$ electrolyte containing 1 M CH$_3$OH at room temperature on Pd/C-N-a-300H and Pt/C-b catalyst. On Pt/C-b catalyst, a large methanol oxidation peak can be clearly observed; while on Pd/C catalyst, there is totally no methanol oxidation current,

Table 3
Calculated bond length and charge densities on each atom of methanol and formic acid

	Bond length (Å)		Bong angle (°)		Atom charge density	
Methanol	1C–2O	1.45278	1C–2O–6H	110.01914	1C	−0.171
	1C–3H	1.09061	2O–1C–3H	105.79343	2O	−0.608
	1C–4H	1.09881	2O–1C–4H	112.37717	3H	0.166
	1C–5H	1.09881	2O–1C–5H	112.37717	4H	0.129
	2O–6H	0.97776	3H–1C–4H	108.61059	5H	0.129
			3H–1C–5H	108.61059	6H	0.355
			4H–1C–5H	108.91112		
Formic acid	1O–2C	1.21873	1O–2C–3O	122.05376	1O	−0.351
	2C–3O	1.37690	1O–2C–5H	123.86411	2C	0.359
	2C–5H	1.10022	3O–2C–5H	114.08213	3O	−0.516
	3O–4H	0.97899	2C–3O–4H	112.95916	4H	0.382
					5H	0.127

indicating that Pd catalyst is almost inactive towards methanol oxidation. So far, it is unclear why Pd/C and Pt/C catalysts represent such different catalytic behaviors to formic acid and methanol oxidation. One possible assumption in the literature is that the site blocking effect due to anion adsorption on Pd may be the main reason for this low catalytic activity for methanol oxidation [27]. Experimental results have shown that both methanol oxidation and formic acid oxidation on Pt proceed via a two-step mechanism, namely initial dissociation adsorption of organic fuel molecules and CO oxidative removal, through the formation of CO_{ads} species as poisoning intermediate. While on Pd metal, a fast direct oxidation is operative for formic acid oxidation and almost no activity for methanol oxidation. To elucidate these different electrochemistry behaviors, the calculated charge densities of each atom in CH_3OH and $HCOOH$ molecules using Becke's three-parameter hybrid functional (B3LYP) with the GAUSSIAN 98 program package [28,29] are listed in Table 3. These calculations are carried out using the 6-31G basis set. It can be found that the charge densities of the elements of carbon and oxygen and hydrogen in these two molecules are

totally different, especially for the carbon atoms. In CH_3OH, it is negatively charged with 0.171, while it is positively charged with 0.359 in HCOOH. Literature research has indicated that methanol molecule is adsorbed on Pt surface with oxygen atom at first and then switched to carbon atom because coordination via carbon atom is more favorable than via oxygen atom [30]. In comparison with valence electron structure of Pt as $5d^9 6s^1$, the negatively charged C atoms in CH_3OH is much more difficult to be adsorbed onto Pd sites than HCOOH because Pd is a poor electron acceptor due to its saturated valence electron structure of $4d^{10}$. It should be noted that charge density of 4H in HCOOH is more positively charged than other atom, which make it more favorable to be adsorbed on Pd to facilitate the following direct oxidation of HCOOH on Pd. Of course, detailed work on the theoretical analysis of the adsorption and desorption behavior of CH_3OH and HCOOH on Pd is needed. Fig. 7 compares the ORR behavior on Pd/C and Pt/C with and without the presence of methanol in the electrolyte. It could be clearly seen that although Pt/C present super ORR performance than Pd/C
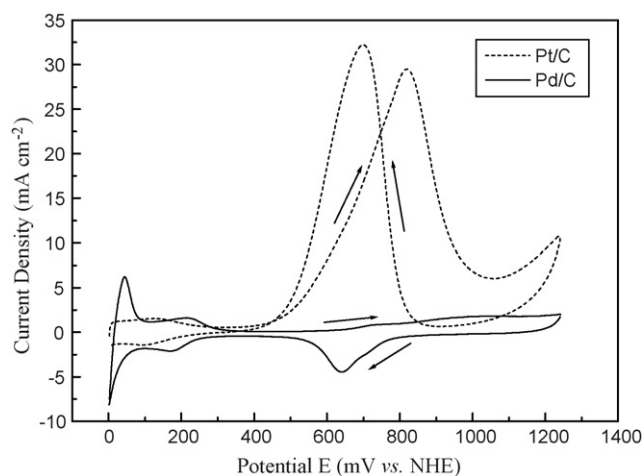

Fig. 6. Methanol oxidation activities on Pd/C-N-a-300H and Pt/C-b catalysts in 0.5 M $HClO_4$ electrolyte with 1 M CH_3OH at room temperature ($25 \pm 0.5\,^\circ C$), the scan rate is 50 mV s^{-1}.
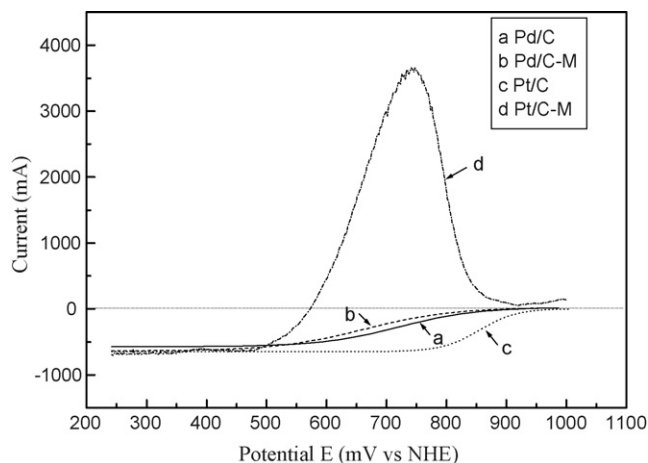

Fig. 7. Current–potential curves for oxygen reduction reaction in O_2 saturated 0.5 M $HClO_4$ containing 0.1 M methanol at a rotating rate of 1600 rpm with a glass carbon electrode employing Pt/C-b and Pd/C-N-a-300H catalysts at $25 \pm 0.5\,^\circ C$. On negative sweep from 1000 mV at a scan rate of 10 mV s^{-1}.

catalyst in pure 0.5 M HClO$_4$ electrolyte; however, in methanol containing solution, ORR on Pt/C is much more deteriorated than on Pd/C catalyst. Much work in the literatures has shown that Pd is inactive to methanol oxidation and presents comparable ORR activity to Pt metal when alloyed with other metals like Fe, Co and Pt [9,10]. If highly active Pd catalyst is employed as the DMFC cathode catalyst, not only the effect of methanol crossover will be decreased, but the utilization of valuable Pt noble metal will be decreased, and thus to decrease the cost of fuel cell to some extent. Considering the important role of Pd nanoparticles in different catalytic regions, this work may open new insights into the exploration of Pd nanoparticles catalyst with high activity and accelerate its application as highly active electro-catalyst in the future.

4. Conclusion

In conclusion, well dispersed carbon supported Pd nanoparticles can be obtained in NH$_3$-mediated polyol process in absence of any protective agent. The average diameter is about 3.4 nm and the size distribution is in the range of 1.5–5 nm if the post-treatment temperature is controlled at 300 °C. Reduction at high temperature up to 500 °C could enlarge the particle size to 5.2 nm and deteriorate the nanoparticles dispersion on the carbon support to some extent. Thermodynamic data analyses display that the added NH$_3$ could control the reaction pathway in polyol process and thus avoid agglomeration of Pd nanoparticles. Theoretical data indicate that the totally different charge distributions in the methanol and formic acid molecules lead to their different oxidation behaviors on Pt and Pd catalysts.

Acknowledgments

References

[1] A.P. Alivisatos, Science 271 (1996) 933–937.
[2] A. Hamnett, Philos. Trans. R. Soc. London A 354 (1996) 1653–1669.
[3] S. Ha, Z. Dunbar, R.I. Masel, J. Power Sources 158 (2006) 129–136.
[4] C. Rice, R.I. Ha, R.I. Masel, P. Waszczuk, A. Wieckowski, T. Barnard, J. Power Sources 111 (2002) 83–89.
[5] R. Larsen, S. Ha, J. Zakzeski, R.I. Masel, J. Power Sources 157 (2006) 78–84.
[6] K. Kinoshita, Electrochemical Oxygen Technology, Wiley, New York, USA, 1992, pp 19–112, 413–414.
[7] A. Capon, R. Parsons, J. Electroanal. Chem. 44 (1973) 239–254.
[8] H.Q. Li, Q. Xin, W.Z. Li, Z.H. Zhou, L.H. Jiang, S.H. Yang, G.Q. Sun, Chem. Commun. (2004) 2776–2777.
[9] M.H. Shao, K. Sasaki, R.R. Adzic, J. Am. Chem. Soc. 128 (2006) 3526–3527.
[10] O. Savadogo, K. Lee, K. Oishi, S. Mitsushima, N. Kamiya, K.I. Ota, Electrochem. Commun. 6 (2004) 105–109.
[11] N. Arul Dhas, H. Cohen, A. Gedanken, J. Phys. Chem. B 101 (1997) 6834–6838.
[12] S.W. Kim, J.N. Park, Y.J. Jang, Y.H. Chung, S.J. Hwang, T.H. Hyeon, Y.W. Kim, Nano Lett. 3 (2003) 1289–1291.
[13] T. Teranishi, M. Miyake, Chem. Mater. 10 (1998) 594–600.
[14] Y. Xiong, J.M. Mclellan, J. Chen, Y. Yin, Z.Y. Li, Y. Xia, J. Am. Chem. Soc. 127 (2005) 17118–17127.
[15] S.W. Chen, K. Huang, J.A. Stearns, Chem. Mater. 12 (2000) 540–547.
[16] H.U. Blaser, H.P. Jallet, M. Muller, M. Studer, Catal. Today 37 (1997) 441–463.
[17] R.W.J. Scott, A.K. Datye, R.M. Crooks, J. Am. Chem. Soc. 125 (2003) 3708–3709.
[18] Y. Wang, J.W. Ren, K. Deng, L.L. Gui, Y.Q. Tang, Chem. Mater. 12 (2000) 1622–1627.
[19] C. Bock, C. Paquet, M. Couillard, G.A. Botton, B.R. MacDougall, J. Am. Chem. Soc. 126 (2004) 8028–8037.
[20] H.Q. Li, G.Q. Sun, Q. Jiang, M.Y. Zhu, S.G. Sun, Q. Xin, Electrochem. Commun. 9 (2007) 1410–1415.
[21] A. Erhan Aksoylu, M. Madalena, A. Freitas, J.L. Figueiredo, Appl. Catal. A: Gen. 192 (2000) 29–42.
[22] V. Radmilovic, H.A. Gasteiger, P.N. Ross, J. Catal. 154 (1995) 98–106.
[23] G. Tamizhmani, J.P. Dodelet, D. Guay, J. Electrochem. Soc. 143 (1996) 18–23.
[24] Z.H. Zhou, S.L. Wang, W.J. Zhou, Q. Xin, G.Q. Sun, Chem. Commun. (2003) 394–395.
[25] J. Luo, L.Y. Wang, D. Mott, P.N. Njoki, N. Kariuki, C.J. Zhong, T. He, J. Mater. Chem. 16 (2006) 1665–1673.
[26] M. Lukaszewski, K. Kusmierczyk, J. Kotowski, H. Siwek, A. Czerwinski, J. Solid State Electrochem. 7 (2003) 69–76.
[27] M. Arenz, T.J. Schmidt, K. Wandelt, P.N. Ross, N.M. Markovic, J. Phys. Chem. B 107 (2003) 9813–9819.
[28] M.J. Frisch, G.W. Trucks, H.B. Schlegel, G.E. Scuseria, M.A. Robb, J.R. Cheeseman, V.G. Zakrzewski, J.A. Montgomery Jr., R.E. Stratmann, J.C. Burant, S. Dapprich, J.M. Millam, A.D. Daniels, K.N. Kudin, M.C. Strain, O. Farkas, J. Tomasi, V. Barone, M. Cossi, R. Cammi, B. Mennucci, C. Pomelli, C. Adamo, S. Clifford, J. Ochterski, G.A. Petersson, P.Y. Ayala, Q. Cui, K. Morokuma, D.K. Malick, A.D. Rabuck, K. Raghavachari, J.B. Oresman, J. Cioslowski, J.V. Ortiz, B.B. Stefanov, G. Liu, A. Liashenko, P. Piskorz, I. Komaromi, R. Gomperts, R.L. Martin, D.J. Fox, T. Keith, M.A. Al-Laham, C.Y. Peng, A. Nanayakkara, C. Gonzalez, M. Challacombe, P.M.W. Gill, B.G. Johnson, W. Chen, M.W. Wong, J.L. Andres, M. Head-Gordon, E.S. Replogle, J.A. Pople, Gaussian 98 (Revision A.6), Gaussian Inc., Pittsburgh, PA, 1998.
[29] A.D. Becke, J. Chem. Phys. 98 (1993) 5648–5652.
[30] B.A. Sexton, A.E. Hughes, Surf. Sci. 140 (1984) 227–248.